First-principles studies on adsorbate-induced faceting of Re(11$\bar{2}$1)

Payam Kaghazchi and Timo Jacob*
Institut für Elektrochemie, Universität Ulm, Albert-Einstein-Allee 47, D-89069 Ulm, Germany

Hao Wang, Wenhua Chen, and Theodore E. Madey
Department of Physics and Astronomy and Laboratory for Surface Modification, Rutgers, the State University of New Jersey, Piscataway, New Jersey 08854, USA
(Received 27 March 2009; published 22 April 2009)

Motivated by our recent scanning tunneling microscopy measurements on Re(11$\bar{2}$1) that, depending on the nature of the adsorbate, showed the formation of distinct facets when the substrate is annealed to elevated temperatures, we used density-functional theory to explore why faceting of Re(11$\bar{2}$1) induced by NH_3 is different from that by O_2. Our calculations indicate that nitrogen adsorption causes two-sided ridges, combining (13$\bar{4}$2) and (31$\bar{4}$2) faces, to become thermodynamically favored at temperatures below 1080 K while oxygen adsorption below 1130 K leads to four-sided pyramids exhibiting (10$\bar{1}$0), (01$\bar{1}$0), (10$\bar{1}$1), and (01$\bar{1}$1) faces.

DOI: 10.1103/PhysRevB.79.132107 PACS number(s): 68.43.Bc, 68.43.Fg, 68.47.−b, 71.15.Mb

Faceted metal surfaces are interesting model systems for studying structural sensitivity and size effects in catalytic reactions.[1–3] Re has mainly been used in the aircraft industry and as catalyst for petroleum processing.[4] Recently, it received increasing interest due to the fact that Re-based catalysts show high reactivity in many important catalytic reactions such as selective reduction of NO_x with NH_3, selective oxidation of methanol, thiophene hydrodesulfurization, and ammonia synthesis, where the reaction rate is sensitive to the catalyst surface structure.[5–10] Particularly, the recent discovery of O-covered faceted Re(12$\bar{3}$1) for the growth of Co nanoclusters demonstrates that adsorbate-covered faceted metal surfaces are also promising templates for synthesis of active model catalysts with high selectivity.[11,12] Besides their catalytic properties, such nanostructured surfaces might provide a basis for bridging the gap between nanoparticles and single-crystal surfaces.[13]

While clean metal surfaces rarely facet, adsorbate-induced faceting of rough surfaces, driven by the anisotropy of surface free energy, is a known phenomenon and has been studied on various systems both experimentally and theoretically.[14–19] Although the driving force for facet formation is believed to be thermodynamics, in most cases this process is hindered kinetically and requires a minimum annealing temperature to occur.

To understand the influence of differently strong interacting adsorbates on the surface morphology of transition metals, we have characterized faceting of Re(11$\bar{2}$1) in the presence of oxygen and nitrogen using low-energy electron diffraction (LEED) and scanning tunneling microscopy (STM).[11] Regarding nitrogen, which was introduced by exposing the system to ammonia at temperatures above 600 K, where it decomposes to leave only N atoms on the surface, the initially planar Re(11$\bar{2}$1) surface becomes completely faceted at 900 K and a pressure of 5×10^{-10} atm. The facets that appear were characterized as ridgelike structures with faces having (13$\bar{4}$2) and (31$\bar{4}$2) orientations (Fig. 1).

However, depositing oxygen at room temperature with exposures less than 30 L, followed by annealing at elevated temperatures, causes the planar Re(11$\bar{2}$1) surface to become partially faceted with (11$\bar{2}$1) and (10$\bar{1}$0) faces forming zigzag chains. Dosing a larger amount of oxygen (exposure $>$100 L) at temperatures between 900 and 1000 K, the surface converts to a morphology with four-sided nanoscale pyramids exposing faces of (01$\bar{1}$0), (10$\bar{1}$0), (01$\bar{1}$1), and (10$\bar{1}$1) (Fig. 2). Since the obtained facet shapes are rather anisotropic, further quantification of the facet sizes still remains difficult. However, the facets resulting from oxygen adsorption on Re(11$\bar{2}$1) are substantially different from those induced by nitrogen.

In this Brief Report, we use density-functional theory (DFT) and atomistic thermodynamics to investigate the surface faceting of Re(11$\bar{2}$1) being in contact either with

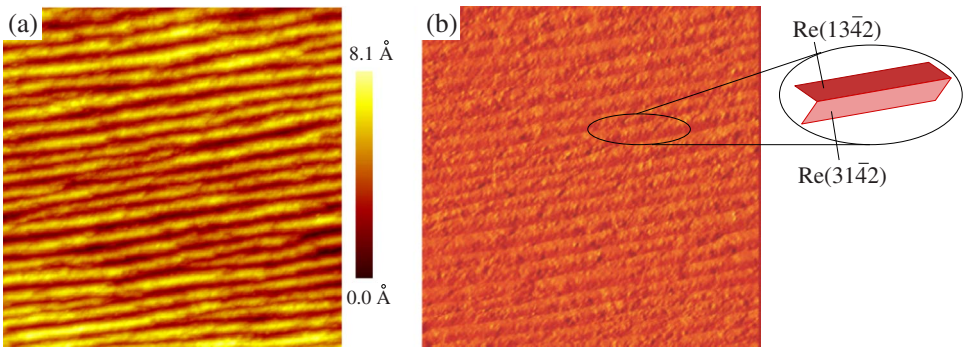

FIG. 1. (Color online) (a) STM and (b) x-slope images of the faceted Re(11$\bar{2}$1) surface prepared by ammonia adsorption (exposure of 300 L) at 900 K. Both figures show a surface area of 1000×1000 Å^2.

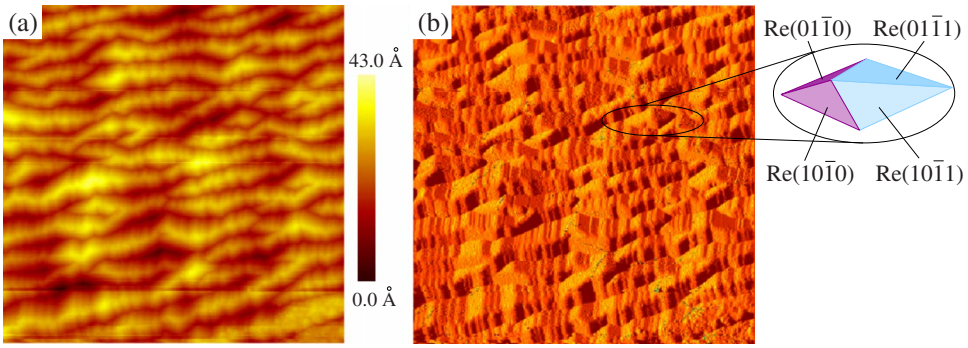

FIG. 2. (Color online) (a) STM and (b) x-slope images of the faceted Re(11$\bar{2}$1) surface prepared by oxygen adsorption (exposure of 300 L) at 1000 K. Both figures show a surface area of 1000×1000 Å^2.

an oxygen or nitrogen atmosphere. The DFT energies for different oxygen or nitrogen overlayers on the surfaces being involved in the facet formations were evaluated using the CASTEP code[20] with Vanderbilt-type ultrasoft pseudopotentials[21] and the generalized gradient approximation exchange-correlation functional proposed by Perdew, Burke, and Ernzerhof.[22] The different surfaces of the initial substrate as well as the faces of the facets were modeled by slab geometries.[23]

When studying facet formation the important quantity is the formation energy, which mainly combines contributions from surfaces, step edges, kinks, and strain. However, when rather extended facets are considered (as in this work), the overall formation energy is dominated by the surface contribution. Then adsorbate-induced faceting occurs under the following condition:[25]

$$\sum_f \frac{S_f}{\cos\,\vartheta_f}\gamma_f^{\text{final}}(T,p_{\text{gas}}) < \gamma^{\text{initial}}(T,p_{\text{gas}}), \tag{1}$$

where S_f and ϑ_f are the partial contribution of face f to each nanoshaped structure and its tilt angle with respect to the initial substrate, γ is the surface free energy, T the temperature, and p_{gas} the partial pressure of the surrounding gas that induces faceting. S_f and ϑ_f can be obtained experimentally but, as far as the facets are well characterized, also by geometric considerations. To study whether a specific nanofacet is formed on the initially planar surface at given p_{gas} and T, the surface free energies of the substrate as well as those of the faces after facet formation need to fulfill relation (1). The facet tilt angles (ϑ_f) and partial contributions to each nanoshaped structure (S_f), given in Table I, were used to generate the corresponding faceting phase diagrams (Figs. 3 and 4).

The free energies of the various surfaces relevant for the faceting were evaluated by the *ab initio* atomistic thermodynamics approach[26–29] that allows investigating of the stability of surfaces being in contact with a surrounding gas atmosphere (reservoir), which is being characterized by a partial pressure p_{gas} and temperature T. Vibrational contributions to γ were estimated for the most stable structures as well as energetically close phases. We found that these contributions do not cause significant modifications in the overall structure of the phase diagram. While, for high temperatures (where desorption occurs), this leads to temperature shifts around 50 and 75 K, considering nitrogen and oxygen adsorptions, respectively, at lower temperatures these contributions are smaller and can be omitted.

In our calculations we used geometrical coverages, which are defined as the number of adsorbed O/N atoms per (1×1) unit cell, thus varying with surface orientation. In comparison, experiments usually use physical coverages, where surface saturation is achieved with 1 monolayer (ML). Unfortunately, there are no direct measurements of saturation coverages on Re(11$\bar{2}$1); but using the highest possible nitrogen/oxygen coverage phases from our calculated phase diagrams (prior to forming the corresponding bulk compounds) to define saturation coverage, we obtain an atom density on Re(11$\bar{2}$1) of 0.89×10^{15} atoms/cm^{-2} for nitrogen and 1.33×10^{15} atoms/cm^{-2} for oxygen. The latter value is in good agreement with the available experimental value of 31.32×10^{15} atoms/cm^{-2} for stepped Re(0001) at 350 K.[30] Finally, this leads to the following approximate conversion between geometrical (GML) and physical monolayers (PML) for the Re(11$\bar{2}$1) substrate: 2 GML-N$\equiv$1 PML-N and 3 GML-O$\equiv$1 PML-O.

Figures 3 and 4 show the surface phase diagrams including clean and nitrogen/oxygen-covered planar or fully faceted surfaces of: (i) the flat Re(11$\bar{2}$1) substrate, (ii) two-sided ridgelike structures with (13$\bar{4}$2) and (31$\bar{4}$2) faces, and (iii) nanopyramids exposing (01$\bar{1}$0), (10$\bar{1}$0), (01$\bar{1}$1), and (10$\bar{1}$1) faces. Any partially faceted surface structure, such as the zigzag chains with (11$\bar{2}$1) and (10$\bar{1}$0) faces observed by STM after oxygen adsorption, were not considered in the phase diagram since these do not represent thermodynamically stable surface phases.

TABLE I. Surface area A [per 1×1-unit cell (calculated)], partial surface contributions (S), and tilt angles (ϑ) for the initial substrate and two types of nanofacets: two-sided ridges consisting of (13$\bar{4}$2) and (31$\bar{4}$2) faces, and four-sided pyramids consisting of (10$\bar{1}$0), (01$\bar{1}$0), (10$\bar{1}$1), and (01$\bar{1}$1) faces. For S the experimentally measured and geometrically derived values are given.

Surface	A (Å^2)	S^{exp}	S^{geo}	ϑ^{geo} (°)
Re(11$\bar{2}$1)	22.54			
Re(10$\bar{1}$0)/(01$\bar{1}$0)	12.43	0.44 ± 0.02	0.456	34.18
Re(10$\bar{1}$1)/(01$\bar{1}$1)	14.11	0.56 ± 0.02	0.544	29.68
Re(13$\bar{4}$2)/(31$\bar{4}$2)	46.77	1.0	1.0	15.42

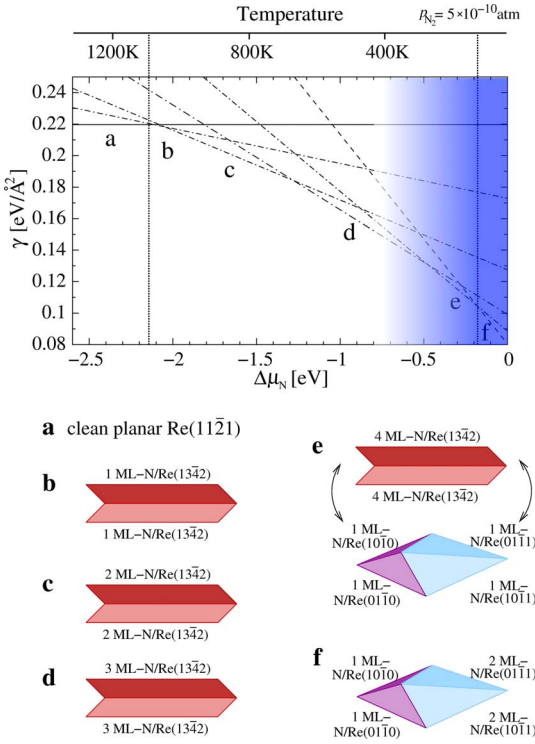

FIG. 3. (Color online) Surface phase diagram for N-induced faceting of planar Re(11$\bar{2}$1) showing the surface free energy as function of the nitrogen chemical potential referenced as $\Delta\mu_N = \mu_N - \frac{1}{2}E^{tot}_{N_2}$. Solid, dot-dashed, and dashed lines represent the planar substrate, two-sided ridges, and four-sided pyramids, respectively.

Prior to discussing the results for N/Re(11$\bar{2}$1), we should mention that experimentally N was deposited on Re(11$\bar{2}$1) using gaseous NH_3, whereas our phase diagram is based on adsorption of nitrogen from N_2. The assumption of a thermodynamic equilibrium with a N_2 atmosphere is justified by the fact that all nitrogen atoms desorbing from the Re surfaces combine to N_2.

Figure 3 shows that, at nitrogen partial pressures of $p_{N_2} = 5 \times 10^{-10}$ atm and $T \geq 1080$ K, no nitrogen is adsorbed on the surface. This temperature is in agreement with the experimental value of 1100 K for desorption of nitrogen from the surface, which according to our calculations should be planar Re(11$\bar{2}$1). For comparison, clean facets of two-sided ridges and four-sided nanopyramids are less stable by 5 and 14 meV/Å^2, respectively. As soon as nitrogen adsorbs below 1080 K, facets become the thermodynamically preferred phase (see Fig. 3). As observed experimentally, the stabilized nanofacets are two-sided ridges, combining Re(13$\bar{4}$2) and Re(31$\bar{4}$2) faces. For the rather large temperature range of 1080 K$>T>$280 K, these nanofacets are significantly more stable than nitrogen-covered planar Re(11$\bar{2}$1) or four-sided nanopyramids with (01$\bar{1}$0), (10$\bar{1}$0), (01$\bar{1}$1), and (10$\bar{1}$1) faces. The latter structure should, from a thermodynamic viewpoint, form below 280 K and above the temperature where a potential Re nitride becomes stable; however, at these low temperatures the kinetic energy for overcoming possible barriers is rather low. Experimental observations proposed that the facets start to form when the nitrogen coverage is larger than 0.4–0.5 PML at 5×10^{-10} atm and temperatures above 700 K. Under these conditions the phase diagram shows phase *c*, which has 2 GML of nitrogen on each face, to be thermodynamically stable. Projecting this coverage onto the Re(11$\bar{2}$1) substrate would lead to 1 GML, which converts to 0.5 PML, being in good agreement with the experimental value. Lowering the temperature (at fixed pressure) does not cause the surface morphology to change but leads to an increase of the nitrogen coverage on the ridges. Although at lower temperatures one would expect a bulk Re nitride to become thermodynamically stable, there is experimental evidence that such a stable compound cannot be obtained directly from the elements.[31] Therefore we only shaded the high $\Delta\mu_N$ range in the phase diagram.

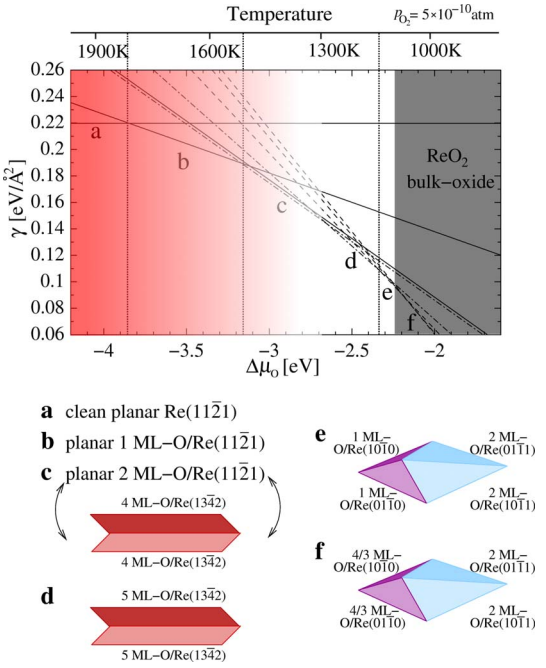

FIG. 4. (Color online) Surface phase diagram for O-induced faceting of planar Re(11$\bar{2}$1) showing the surface free energy as function of the oxygen chemical potential referenced as $\Delta\mu_O = \mu_O - \frac{1}{2}E^{tot}_{O_2}$. Solid, dot-dashed, and dashed lines represent the planar substrate, two-sided ridges, and four-sided pyramids, respectively.

An analogous phase diagram was generated for oxygen-induced faceting of Re(11$\bar{2}$1) (Fig. 4). It shows that, above 1800 K and at the experimentally used oxygen partial pressure of $p_{O_2} = 5 \times 10^{-10}$ atm, desorption of oxygen should occur. This high temperature is certainly related to the strong binding energy of oxygen to the Re(11$\bar{2}$1) surface (3.85 eV per 1/2 O_2) and is consistent with the experimental observation that oxygen desorption starts at $T>1300$ K. Despite this qualitative agreement, further discussion is omitted here since at these rather high temperatures entropy contributions that have been neglected for the adsorbed atoms might affect any conclusion obtained from the phase diagram. At lower temperatures ($T \leq 1130$ K) oxygen-covered two-sided ridges with Re(13$\bar{4}$2) and Re(31$\bar{4}$2) faces, as well as the four-sided

nanopyramids with $(01\bar{1}0)$, $(10\bar{1}0)$, $(01\bar{1}1)$, and $(10\bar{1}1)$ faces show comparable surface free energies, deviating by $2-3$ meV/Å^2, which is within the accuracy of our calculations. While according to the phase diagram the oxygen coverage on Re$(13\bar{4}2)$ and Re$(31\bar{4}2)$, forming the two-sided ridges, is 5.0 GML (0.83 PML on the substrate), in case of the four-sided pyramids both $(01\bar{1}1)$ and $(10\bar{1}1)$ faces are covered with 2.0 GML oxygen, and both $(01\bar{1}0)$ and $(10\bar{1}0)$ faces with 1.0 GML. The latter pyramids were also observed by our experiments at 900 K (see Fig. 2). At this temperature the energy difference between the four-sided pyramids and the two-sided ridges becomes more pronounced (see Fig. 4) with a clear favor for the four-sided nanopyramids. However, according to our calculations ReO_2 bulk oxide becomes thermodynamically stable already below 1100 K. Thus, the experimentally observed structure at 900 K might represent a metastable phase possibly stabilized due to kinetic limitations in the formation of ReO_2 bulk oxide.

Regarding the morphology of the oxygen-induced four-sided nanopyramids, our LEED studies showed that the $(01\bar{1}1)$ and $(10\bar{1}1)$ faces seem to be (2×1) reconstructed.[11] Although in both theoretical phase diagrams (Figs. 3 and 4) the four-sided facets are based on unreconstructed $(01\bar{1}1)$ and $(10\bar{1}1)$ faces, our recent DFT calculations showed that at high adsorbate coverages a (2×1) reconstructed O/Re$(01\bar{1}1)$ surface with a missing-row structure has a comparable surface energy as unreconstructed O/Re$(01\bar{1}1)$. Therefore, our calculations qualitatively support the experimental observation of four-sided nanopyramids exhibiting (2×1)-reconstructed $(01\bar{1}1)$ and $(10\bar{1}1)$ faces.

In order to investigate the sensitivity of our results on choosing a different *xc* functional, the corresponding phase diagrams were also evaluated on the basis of the local-density approximation (LDA). Although with the LDA functional all phase transitions are shifted toward higher temperatures for both oxygen and nitrogen adsorptions (by $\approx$300 K), the overall phase ordering and therefore the conclusions drawn above remain unchanged.

In conclusion, a combination of theoretical calculations and experiments on the adsorbate-induced faceting of Re$(11\bar{2}1)$ are presented. Our DFT calculations not only reproduce the experimentally observed surface faceting but also provide quantitative information and physical insights into the morphological changes of the facets with adsorbate, adsorbate coverage, and annealing temperature. We could show that, by choosing an appropriate adsorbate and environmental temperature and pressure conditions, Re$(11\bar{2}1)$ could be fully faceted with either two-sided ridges or four-sided pyramids. Our work has important implications for Re-based catalysts that operate under oxygen-rich or nitrogen-rich conditions since the structures of the catalysts often affect their performance. We believe that this might stimulate further experimental work using these surfaces as model systems for catalytic studies or as templates for growing nanostructures.

The authors acknowledge support from the German Academic Exchange Service (DAAD) and the "Deutsche Forschungsgemeinschaft" (DFG). The Rutgers authors gratefully acknowledge support from the U.S. Department of Energy.

*timo.jacob@uni-ulm.de

[1] W. Chen *et al.*, J. Am. Chem. Soc. **127**, 5014 (2005).
[2] W. Chen *et al.*, Langmuir **22**, 3166 (2006).
[3] W. Chen *et al.*, J. Phys. Chem. C **112**, 19113 (2008).
[4] A. V. Naumov, Russ. J. Non-Ferrous Metals **48**, 418 (2007).
[5] I. E. Wachs *et al.*, J. Catal. **160**, 322 (1996).
[6] Y. Z. Yuan *et al.*, Chem. Commun. (Cambridge) **2000**, 1421.
[7] J. Liu *et al.*, Catal. Lett. **120**, 274 (2008).
[8] M. E. Bussell *et al.*, J. Catal. **110**, 423 (1988).
[9] M. Asscher *et al.*, J. Catal. **98**, 277 (1986).
[10] R. Kojima *et al.*, Appl. Catal., A **246**, 311 (2003).
[11] H. Wang, Ph.D. thesis, Rutgers University, 2008.
[12] M. Reyhan, H. Wang, and T. E. Madey, Catal. Lett. **129**, 1 (2009).
[13] P. Kaghazchi *et al.*, Faraday Discuss. **140**, 69 (2008).
[14] T. E. Madey *et al.*, Proc. Natl. Acad. Sci. U.S.A. **99**, 6503 (2002).
[15] H. Wang *et al.*, Phys. Rev. B **74**, 205426 (2006).
[16] J. S. Ozcomert *et al.*, Phys. Rev. Lett. **72**, 258 (1994).
[17] Q. Chen and N. V. Richardson, Prog. Surf. Sci. **73**, 59 (2003).
[18] J. G. Che *et al.*, Phys. Rev. Lett. **79**, 4230 (1997).
[19] R. Stumpf, Phys. Rev. Lett. **78**, 4454 (1997).
[20] M. D. Segall *et al.*, J. Phys.: Condens. Matter **14**, 2717 (2002).
[21] D. Vanderbilt, Phys. Rev. B **41**, 7892 (1990).
[22] J. P. Perdew *et al.*, Phys. Rev. Lett. **77**, 3865 (1996).
[23] A plane-wave basis set (E_{cutoff}=380 eV) was used for all surfaces. The Brillouin zones of the (1×1)-surface unit cells of Re$(11\bar{2}1)$, Re$(13\bar{4}2)$, Re$(10\bar{1}0)$, and Re$(10\bar{1}1)$ were sampled with (4×4), (3×3), (5×8), and (4×8) Monkhorst-Pack *k*-point meshes. These surfaces were represented by 19-layer, 30-layer, 11-layer, and 14-layer slabs, respectively, separated by at least 13 Å of vacuum. For the Re$(11\bar{2}1)$, Re$(10\bar{1}0)$, and Re$(10\bar{1}1)$ slabs, the bottom four layers and, for Re$(13\bar{4}2)$, the bottom 14 layers were fixed at the calculated bulk-crystal structure, respectively. Inaccuracies of γ related to slab thickness, vacuum size, plane-wave cutoff, and *k*-point mesh were checked to be <8 meV/Å^2. By comparing to a full-potential all-electron approach [here WIEN2K (Ref. 24) the uncertainties related to the pseudopotentials were estimated to be only $2-4$ meV/Å^2.
[24] P. Blaha *et al.*, *WIEN2k–a Full-Potential Linearized Augmented Plane-Wave Package for Calculating Crystal Properties* (Technische Universität Wien, Austria, 2001).
[25] T. E. Madey *et al.*, Chem. Soc. Rev. **37**, 2310 (2008).
[26] E. Kaxiras *et al.*, Phys. Rev. B **35**, 9625 (1987).
[27] M. Scheffler, *Physics of Solid Surfaces* (Elsevier, Amsterdam, 1987).
[28] G.-X. Qian *et al.*, Phys. Rev. B **38**, 7649 (1988).
[29] K. Reuter and M. Scheffler, Phys. Rev. B **65**, 035406 (2001).
[30] R. Pantel *et al.*, Surf. Sci. **83**, 228 (1979).
[31] P. Clark *et al.*, Appl. Catal., A **184**, 175 (1999).